National Research Council,
Ottawa, ON

Department of Aerospace

Master's internship project

High Lift Noise Reduction with Carbon Nanotubes Thermophones

Authors
Giovanni Landriscina
s1766708

Supervisors
Jerry Syms
Kees Venner

This report has been written during my second year of master in Mechanical Engineering at the University of Twente. From the 5th of September 2017 until the 29th March 2018 I have been working at the National Research Council of Canada, in Ottawa. Here I was working with Dr. Jerry Syms on a **High lift noise reduction with carbon nanotube thermophones** project, where the main goal is to reduce to noise pollution due to the airframe.
The department boasts different labs, like the *e-lab* for electronic works, a carpentry with modern facilities, 4 wind tunnels each for different conditions and dimensions, a testing room to control and monitor the test ran in the wind tunnels, a calibration room to set and calibrate different devices.
I worked mainly alone, under the supervision of Dr. Jerry Syms.
A significant help was given by Shawn Fletcher, especially for the electronic part of my internship and Lynda Smith for the organization.

In order to understand the problem, a soundproofed wind tunnel has been used where to place a simplified model of a landing gear. The pressures have been measured and analyzed in order to understand the fluctuation phenomena linked to the noise field, hence a deeper analysis on carbon nanotubes have been made in order to induce a destructive interference on the noise field.
During this experience I improved my skills to model with SolidWorks, in order to obtain a 3D printed model. Coding with Arduino to control stepper motors needed to have a more precise and better checkup on the experiments, hence to use instrumentations and tools to assemble all the parts needed fro the experiments.
A new developed knowledge about acquisition data system has also been improved, nevertheless how to face drawbacks during the set up into the wind tunnel.
Another important experience I gained was into analyze and understand the material needed and order them to different suppliers.
A Matlab skills was required, nevertheless Ansys-Fluent in order to compare experimental data with the analytical ones.

Abstract

One of the main problem due to the presence of airports close to urban centers is the noise.
Since the engines have been optimized in order to reduce the emission of noise, a considerable source of sound comes from the aerodynamics phenomena. In particular, the main area of the airframe where the noise is produced are the landing gear and the flaps [1].

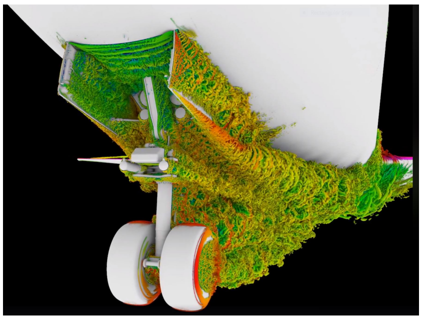

Figure 0.1: Noise simulation by NASA. Image credit: NASA's Ames Research Center, Patrick Moran; NASA's Langley Research Center, Mehdi Khorrami; Exa Corporation, Ehab Fares.

Here at the National Research Council of Canada, the main research center of the country, in the department of aerospace, one of the several challenges is to help to investigate and to reduce the noise pollution.
The center has several wind tunnels, where tests can be performed, especially in winter, where temperature are extremely low and can simulate realistically the atmospheric conditions for flights at considerably altitude.
One of these wind tunnel has been designed and build by Dr. Jerry Syms. It has the particularity to be soundproofed, hence the external noise and any sound reflections will not spoil the experiments.
Considering the Buckingham Theorem, or π-theorem, the problem of a flow around a landing gear of a commercial airplane can be reduced to a simplified model, decreasing considerably the domain, and having a cheaper and much easier structure on which work. The landing gear can be reduced to a couple of cylinders, whom centers lay on the axes parallel to the flow. This configuration allows unsteady vortex shedding to occur in the inter-gap region between the cylinder [2].
The theorem asserts that an equation, or a set of equations as can be Navier-Stokes equations, is described by n physical variables and k physical dimensions, the problem can be reduced in term of $p = n - k$ dimensionless variables. In other words, the problem,

once being dimensionless, match the same conditions independently from the domain.
The first challenge then is to design a proper model. The main dimensionless number to take into account for this project is the Reynolds Number (Re). As a reliable value it has been taken a minimum value Re=22000 [3] .
Hence the model is designed in order to satisfy the turbulence regime, and reproduce at the best the aerodynamic phenomena that occurs on a landing gears.
Studying the flow field and the pressure fluctuations around the body is possible then to predict and to analyze the source of the noise, and therefore act to obtain the desired results.
Previous methods have already been tested [2], therefore a good comparison model can be used.
The idea is to apply carbon nanotubes, a material with high conductivity properties [4], to induce destructive interference and reduce the noise generated by aeroacoustic phenomena occurring on the body.

Figure 0.2: Soundproofed Room at NRC/CRNS designed and built by Dr. Jerry Syms where all the experiments have been tested during my internship.

Contents

List of Figures

List of Tables

Symbol	**Meaning**
NRC-CNRC	National Research Council
Re	Reynolds Number
CNT	Carbon NanoTubes
A	Amplitude
f	frequency
p_0	Reference Pressure
p_t	Total Pressure
C_l	Lift Coefficient
C_d	Drag Coefficient
C_p	Pressure Coefficient
C_s	Heat Capacity per unit area of the conductor
r	distance from the CNT
ρ_0	density of the ambient gas
T_0	Temperature of the ambient gas
α	Thermal diffusivity of the ambient gas
k	Thermal conductivity of the ambient gas
p_{rms}	Root mean square of the sound pressure
β_0	Rate of heat loss

1 Introduction

The NRC's Aerospace Research Center helps the Canadian Aerospace industry with facilities, industry and competence which converge in new ideas, technologies and innovative developments in order to satisfy the market challenges and the needs in the global aeronautic and space sector [5].
The center claims many collaboration with some of the most important organizations and companies of the country like:

- Canadian Space Agency
- Defence Research and Development Canada
- Atomic Energy of Canada Limited
- Canadian Institute of Health Research
- Natural Science and Engineering Research Council

The NRC's Aerospace Research Centre conducts research and technology development across the full spectrum of issues related to the design, manufacture, qualification, performance, use and maintenance of air and space vehicles. This work covers all of the major concerns in aerospacecost, weight, safety, and most recently, environmental footprint. The development and delivery of demonstrated technologies into the aerospace market can best be achieved by combining expertise and resources, and maximizing opportunities for Canadian companies at all levels of the supply chain. In this respect, the NRC's Aerospace Research Center plays a critical role in supporting its collaborators bridge the gap between innovation and commercialization and facilitating the introduction of new technologies into both civilian and military markets.
Indeed the NRC-CNRC can be defined as a bridge between Universities and Companies, where new innovations and developments are explored; taking into account the needs of the market, applying new technologies to real and daily situations.

The Aerospace department at NRC-CNRC provides solutions for different branches of the market:

Aeronautical Product Development Technologies Accelerating the development of new technologies and bringing them to market more rapidly.

Air Defence Systems Reducing the acquisition, maintenance and operating costs as well as the environmental footprint of air defence operations.

Civilian Unmanned Aircraft Systems Supporting the emergence of unmanned flight into the commercial aviation sector.

Reducing Aviation Icing Risk Detecting and mitigating icing risks to meet new regulatory requirements, reduce operational costs and improve flight safety.

Working and Travelling on Aircraft Improving working and traveling onboard aircraft.

The NRC's Aerospace Research Centre focuses on advancing aerospace research and technology developments in the core areas of aerodynamics, flight research, gas turbines, structures and materials, and manufacturing. It also offers a number of research and technical services that include fee-for-service testing, calibration and consulting support.

In the midst of profound changes to the structure of the global aerospace supply chain and a worldwide race to design and manufacture the next generation of aircraft, the NRC's Aerospace Research Centre offers many strategic advantages to Original Equipment Manufacturers (OEMs), Tier 1 suppliers, small and medium-sized enterprises as well as other government departments, universities and research and technology organizations.

They also offer to their clients unique opportunities to participate in large-scale technology demonstration projects, creating important links between players across the Canadian supply chain and ensuring that Canadian companies remain competitive as the industry transitions from current aircraft into radically new aircraft platforms.

The NRC's Aerospace Research Centre has a long history of conducting research, performing technical services and developing technology solutions to support the Canadian aerospace industry.

The clients and collaborations come from all over the world to tap into our extensive pool of highly sought after and specialized staff that includes technical experts, researchers, test pilots, atmospheric scientists, aerodynamicists, structural dynamicists, physicists, metallurgists, software designers, instrumentation and signal analysis specialists, icing experts, programmers, and engineers in the fields of aerospace, airworthiness, chemistry, structures, materials, systems, manufacturing automation and human factors.

Here different fields are dealt that can link aerospace activities to other key sectors including construction, surface transportation, energy, agriculture, and security and disruptive technologies, to name a few. The broad spectrum of disciplines across NRC can help move technologies forward, and the exchange of ideas between areas of research within the same organization allows for rapid technological advancements in new and exciting sectors [5].

1.0.1 The internship in general

The noise generated by a bluff body wake interference is important since it occurs in a wide range of applications as indeed aircraft landing gears, but also industrial heat exchanger and many architectural situations.
As explained before, the noise produced by a airplane during the landing comes more from its airframe than from its engines [2].
Since the sound emitted from the engines has been reduced considerably [1], the next challenge is to act on the airframe to reduce the noise pollution which can cause many discomforts to the people who work and live next to airports.

At the NRC-CNRC, in the aerospace department, Dr. Syms has been trying to use Nanotubes of Carbon to apply on landing gears in order to tackle this aeroacoustic problem.

Acting on the origins of the pressure fluctuation induced by a Von Karman [6] effect, which causes a noise generation, inducing a destructive interference the sound can ideally reduced.

One may claim to change the design of the landing gears or to add aerodynamics surfaces in order to avoid those phenomena, but one of the main purpose of these bodies (landing gears and flaps) is to increase the drag resistance during the landing phase and help the vehicle to slow down.
Indeed the noise emitted and the drag effects are strictly correlated, hence the CNTs method to face the problem has not to be aerodynamically invasive.

2 Background

2.0.1 Sound Pressure Level

First of all is necessary to understand how the flow field facing an object can produce noise.
As basic example it might be taken a musical instrument as the trump or a flute, where the flow air (the breath of the player) passes through the body (instrument) generating sound.
The sound indeed is the result of the vibration of the molecules in the air, this movement is periodic and it is linked to a series of a repeating pattern of high-pressure and low-pressure regions moving through a medium, it is sometimes referred to as a pressure wave The sound, which is measured in decibel [dB], is then directly connected to the pressure variation through a medium and it can be measured thanks to the definition of **Sound Pressure Level** (SPL) [7]:

$$SPL = 20log_{10}\left(\frac{p}{p_0}\right) dB \tag{2.1}$$

Where and p_0 [Pa] is the reference pressure and p [Pa] is the root mean square (RMS) sound pressure, which for a simple sin wave $y = A_1 sin\left(2\pi f t\right)$ is:

$$RMS = \frac{A1}{\sqrt{2}} \tag{2.2}$$

In this way the pressure on the body is a good indicator of the source of the noise [7].
In order to monitor the noise reduction the Power Spectral Density is introduced. It defines the distribution of the power of a signal over the frequency. Therefore, allows to identify the frequency on which the power of the signal has more influence of the overall signal.
A knowledge of Fourier Transform is needed in order to switch a signal from the time domain to a frequency domain, and therefore analyze its spectrum and identify the frequencies on which act.

2.0.2 Von Karman effect

As explained before, the pressure wave occurs when during the domain high and low pressure alternate each other. It means that there is a periodicity during the time of

oscillating pressure [6].
That can be explained by the Von Karman effect. It describes the oscillating behavior of the flow when it faces a symmetric surface, in this case a cylinder. After an initial phase of transition, when the flow downstream is still symmetric respect the axis of along the flow, instabilities appear causing a periodic oscillation of the flow.
It hence brings to a areas of high pressure, whereas low pressure symmetrically to the axis.
The phenomena has been simulated by analytical solutions (OpenFoam or Ansys) (fig. 4.13).

2.0.3 Carbon Nanotubes

Here at the National Research Council in order to tackle this problem is to use **Carbon NanoTubes**.
This material has been a discovered in 1952 by Radushkenich and Lukyanovich, which obtained Nanotubes in Carbon with a 50 nanometers of diameters‘[8]
.

Subsequently, in 1992 was for the first time theorized the electronic properties of single-walled carbon nanotubes at the Naval Research Laboratory at the MIT[9]

Only in 2008 at the *Department of Physic & Tsinghua-Foxconn Nanotechnology Research Centre* in Beijing a group of researchers described the acoustic properties of this material.

In particular, a very thin layer of carbon nanotube films, due to its extremely high conductivity, fed by sound frequency electric current can emit loud sounds. This is phenomena is due to a thermoacoustic effect[4].
Indeed the high conductivity of this material when it is crossed by an alternating current heats the CNTs, resulting in a temperature oscillation which excites the the pressure oscillation in the surrounding area, causing a sound generation.
It has to make clear that what generates the sound is the expansion and the contraction of the air in the vicinity and not the mechanical movement of the CNTs, which do not show any relevant thermal expansion. The extremely advantages of this material are:

- The flexibility , which allows the thin layer film to be tailored to different shapes and sizes, freestanding or placed on different surfaces; nevertheless they are stretchable and transparent [4]
- They are magnet-free and without moving parts, what a normal loudspeaker is not [4].

In particular, the experiment conducted was focused on two different CNTs loudspeaker films: one just using one layer and a second one with four layers.
In this way, increasing the thickness, the resistance proportionally decreases. Applying a

sinusoidal voltage across the electrodes on which the CNTs are directly placed, a loud tones emitted can clearly heard.
What has be found from this experiment is how, despite the excellent performance of the CNTs loudspeaker, the output frequency doubles the input 2.1.

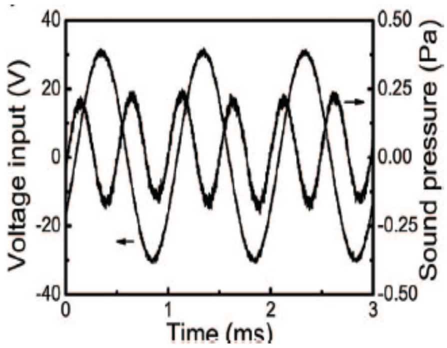

Figure 2.1: Real time signal of the input voltage of the four-layer CNT thin film loud speaker and the output sound pressure from the microphone. The frequency out the sound pressure is double than the input voltage [4]

.

The sound emitted has been previously studied by Arnold and Crandall [10], which described the sound pressure emitted by a thermophone in relation to the input power. For the CNTs the same study has been done, taking into account the rate of heat loss per unit area of the thin layer due to conduction, convection and radiation β_0.
According to [4], the sound pressure emitted by a thermoacoustic thin film loudspeaker has the following form:

$$p_{rms} = \frac{\sqrt{\alpha}\rho_0}{2\sqrt{\pi}T_0}\frac{1}{r}P_{input}\frac{\sqrt{f}}{C_s}\frac{\frac{f}{f_2}}{\sqrt{\left(1+\sqrt{\frac{f}{f_1}}\right)^2+\left(\frac{f}{f_2}+\sqrt{\frac{f}{f_1}}\right)^2}} \tag{2.3}$$

Where:

$$f_1 = \frac{\alpha\beta_0^2}{(\pi k^2)}; \quad f_2 = \frac{\beta_0}{(\pi C_s)} \tag{2.4}$$

The theoretical results vs the experimental are given in fig. 2.2

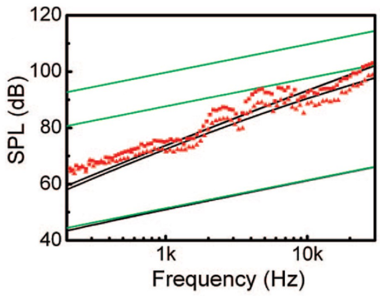

Figure 2.2: In black the theoretical data from equation 2.3, (the upper one is for one-layer, the lower one for a four-layers, while the red dots are the experimental data (squared for one-layer, triangles for four.layers). The green lines are calculated using the Arnold and Crandall's theory)

2.1 Related work

Different previous works have been used to first understand the problem, and then analyzed into the details.

- The guide line to set the experiment has been given by a work in collaboration between the *University of Notre Dame, Indiana USA* and the *Kumoh National Institute of Technology, Gyeonbguk Korea* [2].
  The researchers worked on a simplified model of a tandem cylinder, built by their own, in order to study the pressure field around the bluff body.
  The geometry and part of the instrumentation is hence taken from this work.
  In this paper a method to reduce the noise generated by a Re between $22'000$ and $172'000$ due to a couple of cylinder is by an emission of plasma.
  It has first investigate the pressure and the pressure oscillation around the up and down stream cylinders first without plasma actuator, and after with it.

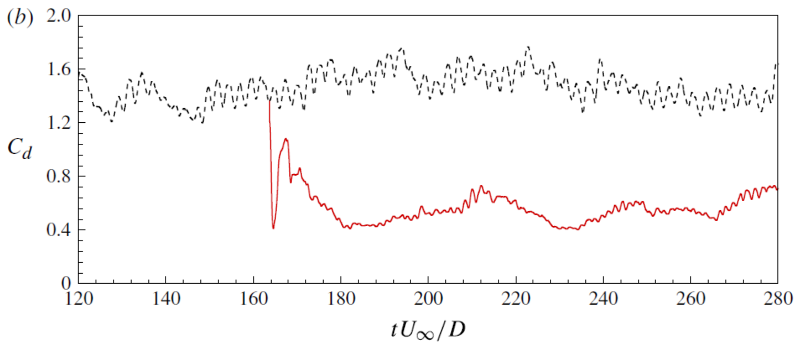

Figure 2.3: The drag coefficient for the downstream cylinder, in black without the plasma actuator, in red with the noise reduction system on.

The results were pretty satisfying, with a side effect of drag reduction fig.2.3.
Indeed a good drag is wanted: the landing gear plays an important role into the reduction of the speed during the landing phase, and the plasma emitted from the downstream cylinder shrinks the aerodynamic resistance.
The researchers also compared the experimental results with the analytical ones with the use of the software *OpenFoam*, using in turn a work done by the *University Of Adelaide, Australia*.

- The work done by *J. Doolan* was focused on the simulation on the same configuration (tandem cylinder, with centers far 3.7D each other) using a OpenFOAM source code[11].
  The experimental data were compared to experimental published data by NASA.
  It is showed how the simulation can approximate pretty good the experimental results, were the difference might be justified by neglecting the the spanwise velocity during the simulation.
  This work gave enough confidence to trust into the simulation of the problem, where it has been used during my internship.
  In particular, the paper shows a simulation made by OpenFOAM to solve the incompressible unsteady Reynolds Averaged Navier Stokes (URANS) ad continuity equations using the k-epsilon turbulence model.
  A second-order discretization method was used for the convective flows, a second-order centered scheme scheme was used for the viscous terms and a second-order implicit method time.stepping method was used to estimate the temporal terms[11].
  Those settings have been used as a first configuration for my analysis, with a different software, which uses the same computational schemes as OpenFOAM.

- An important work about CNTs has been done at the *Univeristy of Beijing*.
  As explained before, this research was focused on the sound properties of this material.
  It is shown how once the CNTs are fed by a electric current, they produce loud sound with a double frequency of the input.
  They also show how the physical properties of CNTs are extremely useful, especially their flexibility and transparency[4].

3 Methodology

As the main reference the work [2] as been taken.
From this work in particular the geometry and the typology of the material has been taken as inspiration in order to build the model.
In order to obtain the turbulence phenomena which generates the desired noise the geometry is extremely important. It has to satisfy several aspects. First of all the physical phenomenas that have to been studied depends on the geometry. The model has to be inserted in a preexisting environment and interact with the instrumentation at the NRC/CNRC, hence the sizes have to fit.
The geometry can also influence desired and undesired mechanical phenomena like: vibrations, breakages or bending.
In parallel the choice of the instrumentation can influence the design: the room and the space to place the instruments into the model can change the geometry; hence a choice of the instrumentation have to made.

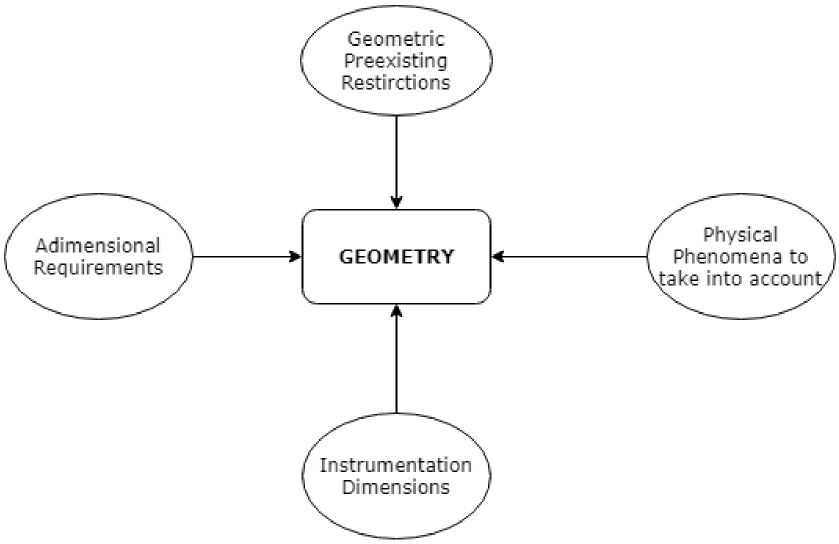

Figure 3.1: Simple scheme of what influences the choice of the geometry in order to design the model

The devices to add on the model are hence chosen while the geometry is developed, in this way the model is much less bulky.
As guide line a good bibliography about the same kind of experiment has been taken

into account, in particular the work from [2].
From those previous works a good starting point to look for a proper material can be obtained.
The combination of it with previous experiences from the researchers at the NRC and with simulations, gives good first idea of the specifics to satisfy.
Another aspect to consider is the controllability of the devices and its precision. In particular an electronic device is favorite over a manually controlled one.
The repeatability of the experiment plays also a role. Same conditions have to be reproduced in order to be able to compare different solutions when specific elements are changed.
Finally a good combination of price and performance leads to chose between different products and different suppliers.

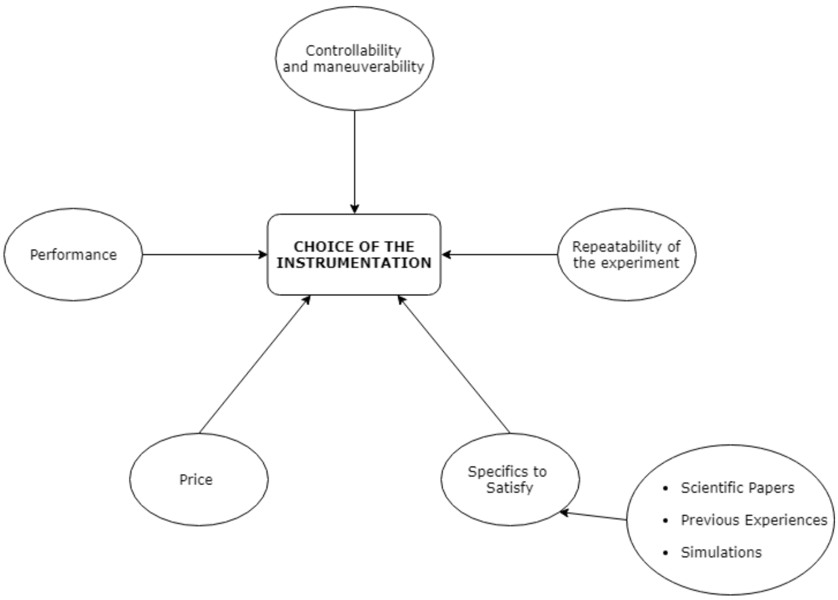

Figure 3.2: Simple scheme that leads to a choice of the instrumentations

Once that the material has been chose, it was ordered by different and suggested suppliers and combined.

3.1 System Decomposition

As explained, the landing gear is reduced to a simpler system which consists of a couple of cylinder whom centers lay on a axis parallel to the flow.
The challenge was to design those cylinders in order to have a proper geometry to obtain a minimum $Re = 22000$ [3] considering atmospheric conditions (T=25C) hence a viscosity

$1.7894e-05\frac{kg}{ms}$ and density $1.225\frac{kg}{m^3}$. From the definition of the Reynolds Number [6], and from a given starting velocity in the soundproofed wind tunnel of $10\frac{m}{s}$, the diameter D of the cylinders is therefore:

$$D = \frac{Re\mu}{U_{\infty}\rho} = 0.033m \tag{3.1}$$

Furthermore the cylinders have to host a flush mounted differential pressure sensors. The cylinders are then hollowed with three mobile parts placed every 120 degrees along the cylinder that allowed us to place the sensor and to slide them along the direction of the axis of the cylinder in order to place them in the flow.
Those cylinders have to be set far each other with a length $L = 3.7D$ and $4D$ [12] and on one side connected to a stepper motor (NEMA17) and on the other side to a bearing. This setting allows the cylinders, hence the pressure sensor, to rotate and to measure the pressure on different angles thanks to the stepper motor controlled by an self implemented Arduino code.
All the model has been first designed with SolidWorks, then printed with a 3D printer. In order to solve different issues due to lack of controllability of Arduino or physical undesired phenomena, other devices have been added or measures have been taken while the set up was in the assembling phase.

3.2 Design Rationale

In order to design a model different aspects have to be considered: the possibility to change the distance between the two cylinders, the room for the pressure sensors, the height which can ensure the flow to pass thought the pressure sensor and a design which can allow the instrumentation to be placed without too many complexities.
Thanks to the help of the modern 3D printers, the model can be first design with the software SolidWorks, then sent by the website **3dHub** printed, and assembled.
The design was split into two parts, first of focusing on the structure that has to host the stepper motors and to sustain the cylinders reducing at the minimum the vibrations. In order to satisfy those specs, the frame has been separated into two parts, a bottom part, with sites which host the stepper motors, and a upper one that allows the cylinders to slide into bearings fitted in the upper frame. Those two parts are then sustained thanks to the supports that have to be strong enough to resist to a strong flow in the wind tunnel and reduce the induces vibration.
The structure then has to be designed in order to change the distance between the cylinders from 3.7D to 4D [12].
In order to save material and avoid to print a new frame, the fixed part of the model has been designed with both configuration.
In this way the configuration can be changed simply rotating by 180 the frames.

Once that the final design was delivered to the printer, on problem came out. The dimension of the frame was slightly exceeding the maximum supported by the printer. In order to make up for these issues, the frame has been reduced in side, adding transversal parts that link the supports to the upper and lower frames.

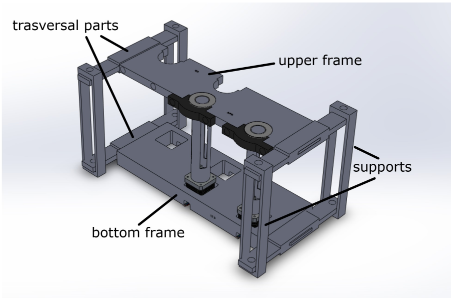

Figure 3.3: 3D view of the model in SolidWorks

The cylinders have the main characteristic to be hollow enough to host a pressure sensor with all the wires and tubes connected to it.
The final design consists into a cylinder with 3 hollow parts, placed 270 from each other, that are filled with sliders that can,indeed, slide along the direction of the axis of the cylinder in order to guarantee the transducer to be into the flow. In this way the setting part of the experiment results less challenging since we deal with dimensions in order of centimeters.
The sliders, on the inner part, show a pocket where the transducer can be placed avoiding any undesired movements, and a hole through which the sensor is flash mounted fig.3.4. Also in this case a problem showed up: the shape of the cylinder could not allow the printer to give a smooth cylinder, inducing many irregularities. To tackle this problem the cylinder were printed without the upper part (fig.3.4) to slide into the bearing, but it was gathered after using acetone, thanks to the property of the ABS, the chosen material. On the bottom of the cylinder 4 holes allow the cylinder to be screwed to the hub, connected to the shaft of the stepper motor.

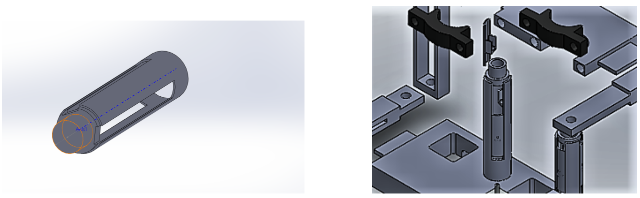

Figure 3.4: On the left the orange part has been printed separately and after gathered with acetone thanks to the properties of the ABS, on the right the unassembled draw of the slider of the cylinder with a site for the pressure sensor.

4 Implementation

In this section the method to implement the set up is explained, hence the choice of the material.
Different programs are used and explained in order to have a better control and feedback on the set up.
Figures of the scripts and of the sketches are present to help to understand better the implementations.

4.1 Printing of the Model

After different consultation with different manufacturers, on the platform available on **3D Hubs**, about the best material, the choice has been made between 3 main materials: ABS, ASA and PLA that show different characteristics:

The main characteristic desired was the smoothness, while the price played also an important role into the choice of the material.

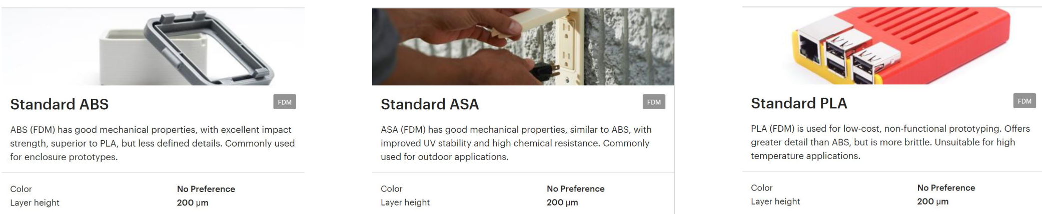

Figure 4.1: General Properties of the three material to choose to print the fianl model

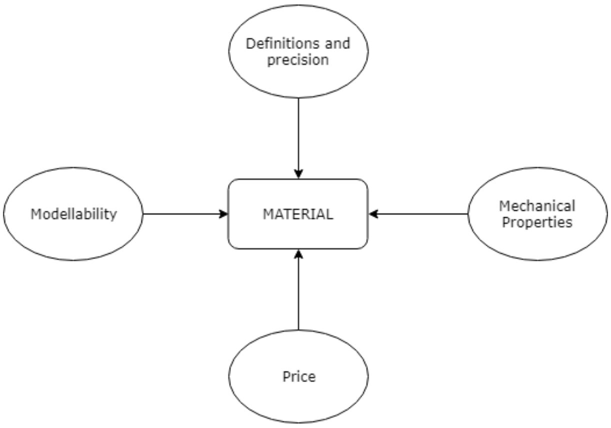

Figure 4.2: Diagram of the main aspects in the choice of the material

Another advantage that induced to choose the ABS is its property to be sanded after the process of printing, hence the smoothness and the precision of different part can be improved.
For the frames, a different material has been used, since the printing of such a big part would have lead to torsional problem: a stronger material like PLA has been chosen for those parts where the precision was not particularly requested.
Once that the model arrived, a sanding process to increase the smoothness of the surfaces and of the connecting parts has been done.
To have the cylinders placed in a way that the flow can cross them, the bottom frame has been screwed on a wood board fig. 4.3

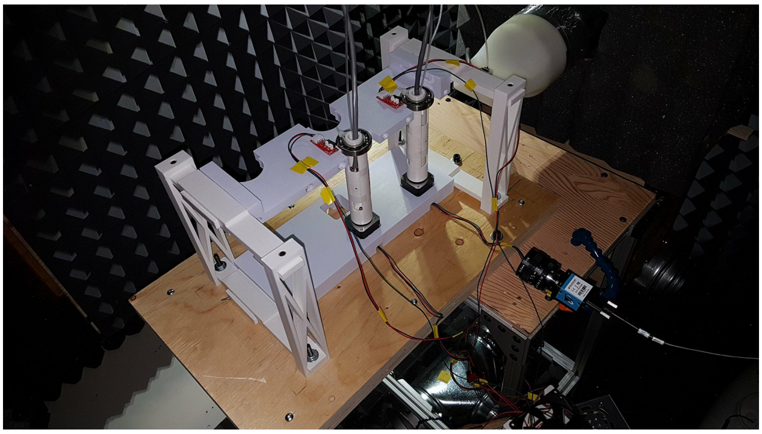

Figure 4.3: Model printed with ABS and PLA, assembled and set into the soundproof wind tunnel

Subsequently all the instrumentation has been added to the model.

4.2 Programming with Arduino

Before fixing the model to the table, as can be seen from the figure 4.3, the stepper motors (NEMA17) fig. 4.4 were inserted in the holes in order to reduce the induced vibrations.
As previously said the stepper motors are controlled with ArduinoUNO to have a complete and accurate pressure field around the cylinders.

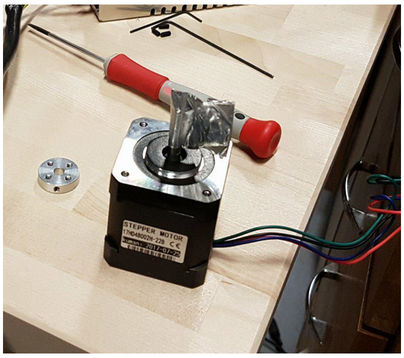

Figure 4.4: NEMA17 stepper motor

ArduinoUNO has an easy language command, called **wiring**, C++/C which is implemented by a so called sketch available from Arduino Application.
The sketch gives simple commands to the pins based on the action wanted by the user, through an USB cable.
The ArduinoUNO is connected to a CNC shield in order to simplify the connection and the command to the stepper motors fig. 4.5.

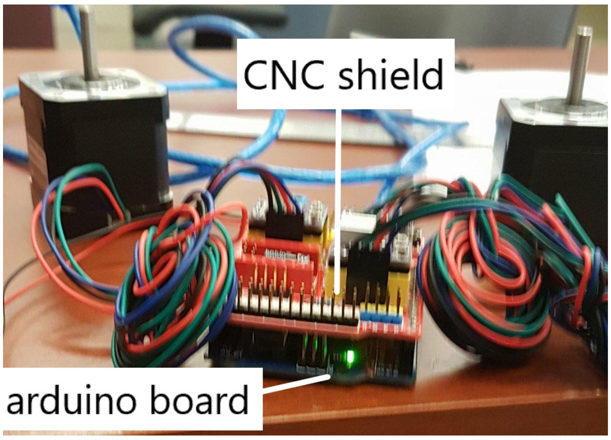

Figure 4.5: Arduino and the CNC Sheild to simplify the connection

The first 7 pins give the digital control of the stepper motor, which are divided into 3 axis, corresponding to 3 motors NEMA17. Since the project consists into 2 cylinders, only 2 stepper motors are controlled.

During the attempts to run the code, a considerably increase of temperature was noticed from the driver.
That was probably due to a high voltage requested by the stepper motors (20V). This demand of voltage was indeed solved with a power supplier.
Connecting to the power supplier a fan, and printing with a 3D printer a frame to host the Arduino driver, the CNC shield and the fan, the overheating problem was solved fig. 4.6.

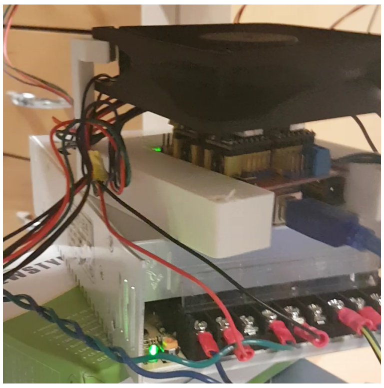

Figure 4.6: Frame to hold the fan to cool the CNC shield. Both are fed by a power supply.

The Arduino software is extremely simple and one of its disadvantage is into the absence of feedback from the stepper motors to the driver, nevertheless the impossibility to stop the sketch if not stopping the power.
The first issue is solved by connecting a limit switcher RAMS 1.4 to each stepper motor. Wrapping on the top of the cylinder a wrapping tie, when the cylinder rotates, it touches the limit switcher screwed on the upper frame.
Since the CNC shield, to which the stepper motors are plugged, has one ground pin and one 5V pin to feed the RAMs 1.4, a jumper has been made, in order to connect simultaneously two limit switches.
A circuit is shown in fig. 4.7

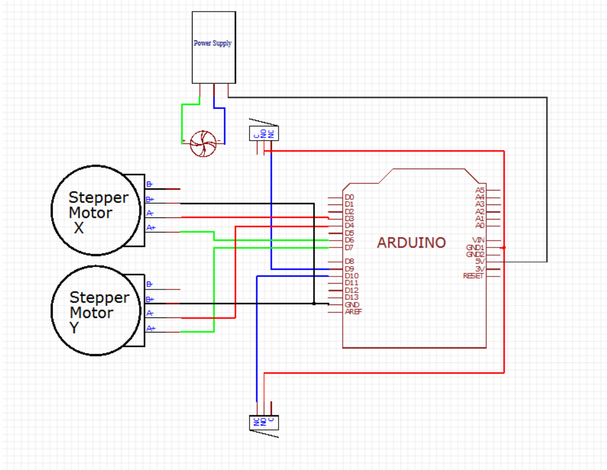

Figure 4.7: Simplified scheme of the connection of the stepper motors to Arduino Uno

The switches are hence fixed to the top of the structure, and give the home position of the stepper motors; in this way the position of the pressure sensors is given.

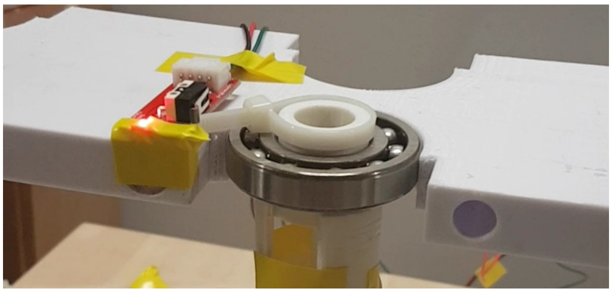

Figure 4.8: Limit Switch on the upper frame gives the zero-position in order to allow the repeatability of the experiment using a cut wrapping tie

The other issue is due to the noise that the stepper motors produce while the Arduino code is running. In order to avoid it, which would spoil the sound recorder by the microphone placed between the 2 cylinders, the power supply is plugged into a power switch. In this way the entire circuit is turned off while the pressures and the sound is recorded.
The simple code is explained in fig. 4.9
The driver and the shield are placed into the chamber, while the USB cable passes through a hole in the wall, allows to control the cylinder from the outside the wind tunnel.

The Arduino sketches in this way allow to control in a more precisely the rotation of the cylinder and to bring them back to the same initial position everytime a new session of the experiment runs.

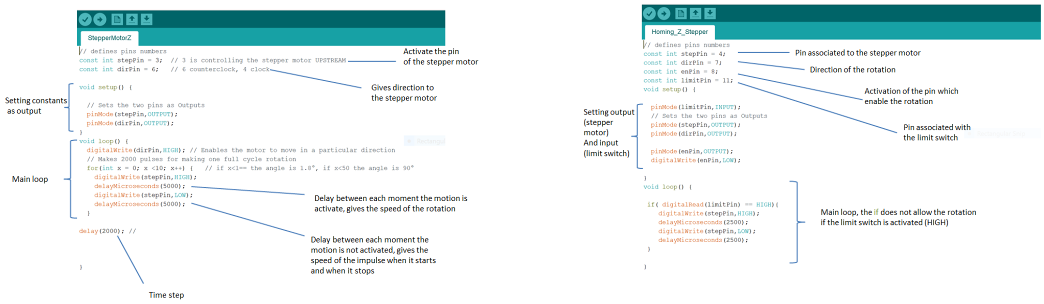

Figure 4.9: On the left the main script for one stepper motor, on the right the sketch to stop the cylinder when it hits the limit switcher

Hence, to move the cylinders one code is used, with a settable delay, long enough to get data. Then to bring the cylinder to its initial position another code is used.
The delay is in *microseconds* units, while the angle to give to control the stepper motor is determined by its step angle, that for a NEMA17 is 1.8 degree.
The input to digit into the Arduino code is hence a ratio:

$$1 : 360 = 1.8 : X \tag{4.1}$$

Therefore when 1 is given as an input, the motor takes one step, which is 1.8 degree. In order to have a Y angle, the input to give is:

$$Input = \frac{Y}{1.8} \tag{4.2}$$

In the example in the fig. 4.9, the input is 10, hence the stepper motor take a step of 18 degrees. To have a rotation of 90 degrees the input has to be 50, for 180 degrees 100 and so on.

4.3 Ansys Analysis

In order to verify the experimental result, a way already proposed by NASA [13] is to descirbe the problem of a bluff body in a uniform flow with a numerical simulation.
In the project [11] used as model the program used was OpenFoam, which was the first choice.
After a first attempt to understand and especially to define the geometry of the problem, in order to save time the choice has switched to Ansys, which is a more intuitive software with the disadvantage of beeing expensive.
The gemotery has been imposted on to the 3.7D configuration [12].

4.3.1 Geometry and Meshing

First of all, Ansys can create a geometry using a layout not so different from SolidWork. After having defined the axis and the flow domain, which is a rectangle, the cylinders are represented in a 2D problem as two circles of 0.033 meters.
The domain has to be specified being a fluid, while the circles are the walls of the cylinders.
IMAGINE GEOMETRY
An important step is to name the regions and the boundaries.
After that the meshing has to be applied.
Since the problem has different geometry in its domain, the accuracy of the mesh has to be increased next to the walls, where the turbulent phenomena are stronger, and a good and high resolution solution is desired.
After applying a first mesh of default, the method has changed into triangles, in order to have a smoother mesh around the cylinders.
After, setting the *size around the cylinders* through the command **element size** and selecting the walls, the size is reduced to $0.0005m$.
In order to have a better precision the **Inflation** is applied on the 1^{st} layer of thickness and on the 1^{st} layer of height, while the size is the same as the element size next to the wall, $0.0005m$.
The maximum layer, which leads to the thickness of the inflation from the cylinder, is set to 15, while the growth rate to 1.5.
Those latter setting depend on the gemoetry mainly, the increase the accuracy of the result but the decrease the speed of the calculation.
The final mesh is shown in the fig. 4.10

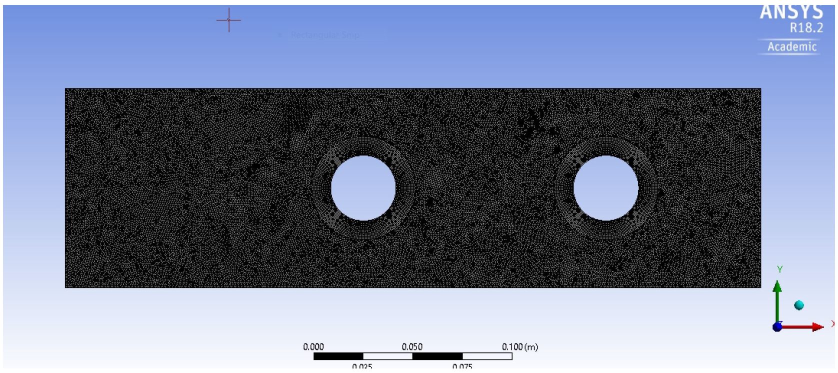

Figure 4.10: Final mesh

4.3.2 Setup

Once that the mesh is applied, the set up gives the physical properties of the problem and the setting by how it has to be solved.

Retaining the pressure by default (atmospheric at 25 C), the model has to changed into Viscous, Large Eddy Simulation typing into the command window **('les-2d? #t')** in that way the Viscous Model is added.

The Setup has been after moved to the fluid, where the air is retained at the default setting:

Table 4.1: Fluid Properties

p_0	101325 Pa
ρ	1.225 $\frac{kg}{m^3}$
μ	1.7894e-05 $\frac{kg}{ms}$
T	25 C

Once that the fluid domain is set, the boundary conditions have to defined: using the names given to the domain, the boundaries are easily defined:
At the **inlet** the velocity is set to $10\frac{m}{s}$, at the upper and lower walls the default condition has not being changed, while on the cylinders the Viscous Method set before already gives the boundary conditions around the bodies.

4.3.3 Solution

Setting the Solution means deciding with which precision and computational effort the problem has to be solved. Still using the advices given in a workshop to study the aeroacoustic phenomena with Ansys [14] , the **Solution Methods** have changed:

1. Retain the default **Least Squares Cell Based** under **Gradient**.
2. Select **PRESTO!** under Pressure discretization
3. Retain default **Bounded Central Differencing** under **Momentum**
4. Select **Second Order Implicit** under **Transient Formulation**.
5. Check **Non-Iterative Time Advancement** option
6. Select **Fractional Step Method** as **Pressure-Velocity Coupling** scheme.

After that, the **Solution** has to be initialized, so under **initialization** checking from the inlet, the problem is ready to be solved.
In order to control that the solution gives an expected trend, under **Monitor** the lift and the drag coefficient can be plotted as the problem is solved during the time steps. Some versions of Ansys have the monitor of this force coefficients already set, in others have to be added. Checking the plot, especially of the lift coefficient of the upstream cylinder, which has a predictable trend, comparing with the theoretical plot can be seen

if the solution gives and expected physical meaning. Indeed the lift coefficient for the upstream cylinder in a uniform flow has the following behavior:

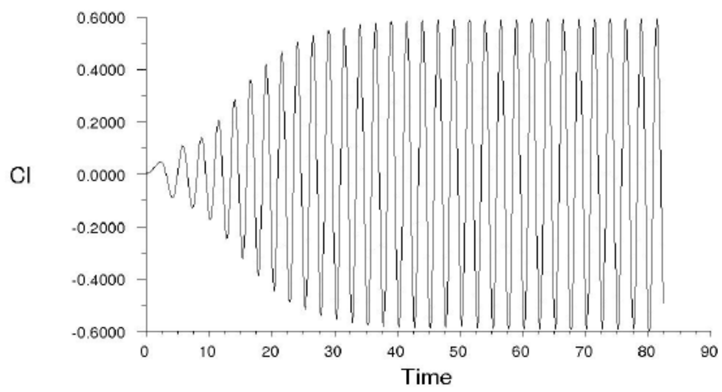

Figure 4.11: Theoretical Lift Coefficient for a cylinder in a uniform flow field, from **Flow past a Cylinder with a Flapping Element Attached to Its End.** - *William W. Liou1, Srinivasa R. Pantula2, Tianshu Liu3, Javier Montefort4, David Ludens5Western Michigan University, Kalamazoo, MI, 49008, USA*

It is hence expected during the simulation that the lift coefficient will assume during the time a shape described in fig. 4.11, when it does not a problem into defined the solution and the setup occurs.
The **Reference Values** have to be set in order to have a proper dimensionless values: velocity $= 10\frac{m}{s}$, Length $= 0.033m$.
After that under **Run Calculation** the parameters to solve the problem are defined: after several attempts, and depending on the power of the calculator the time to run the simulation the solving parameters are set:

Table 4.2: Solving Parameters

Time Step	0.001
Number of Steps	1000
Max Iterations per Time Step	20
Ending Time [s]	1

In order to save the solution and having the results for each time step, under the section checking ....
in this way Ansys can save and give the solution and any time step desired.

Once that everything is set, the simulation can start. The final lift coefficient given is shown in fig. 4.12

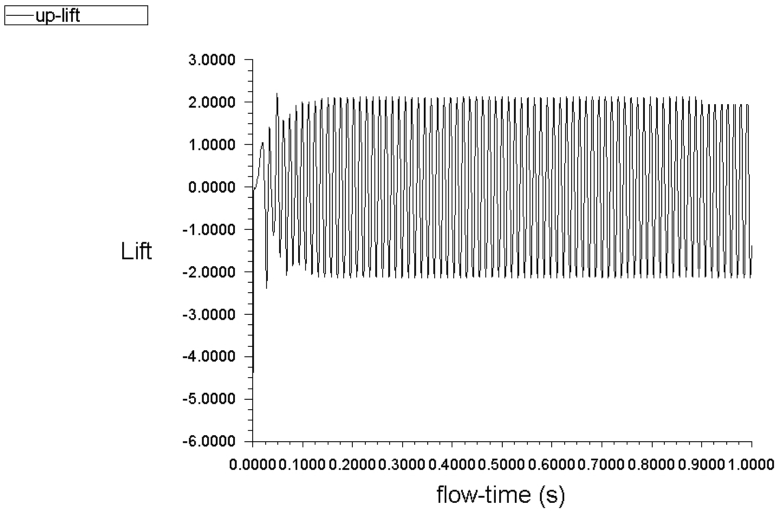

Figure 4.12: Lift Coefficient for the upstream cylinder obtained from Ansys simulation to monitor the solution

As can be seen, the lift coefficient has the expected behavior, hence the solution is accepted.

4.3.4 Results

Once that the solution is given, the Results using **Fluent** can be obtained.
A map of the velcoity and the pressure field obtained by Fluent is in the fig. 4.13

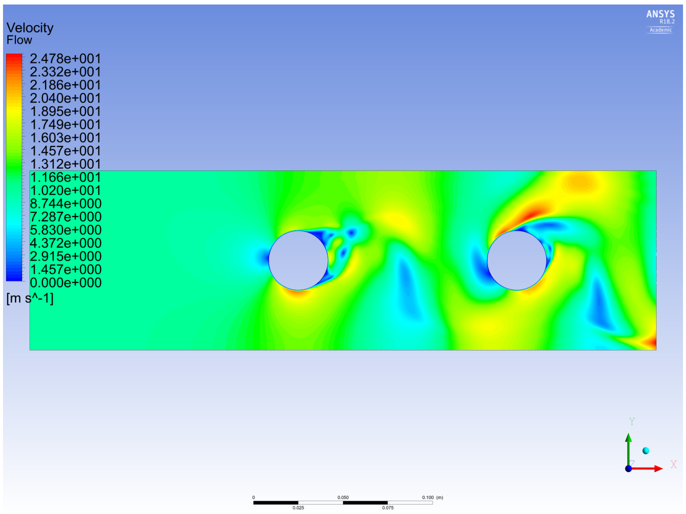

Figure 4.13: Velocity field around the 3.7D configuration

From the velocity field can be observed how the Von Karman effect are produced behind the upstream cylinder and how those oscillating phenomena affect so much the flow field around the downstream cylinder, causing a considerable variation of the pressure field around it.

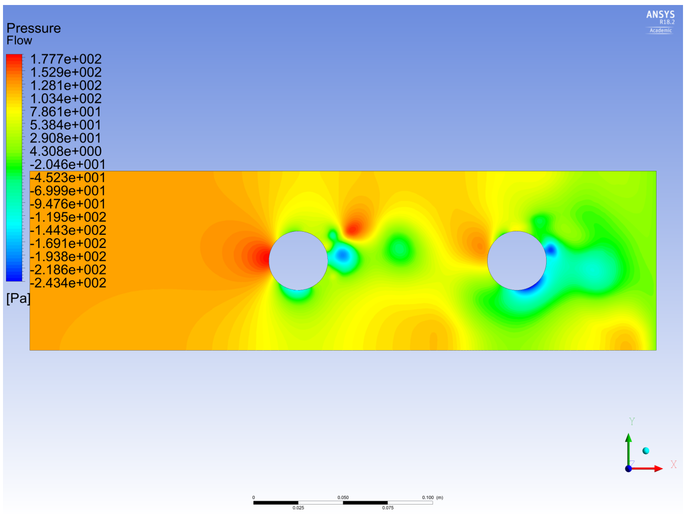

Figure 4.14: Pressure field around the 3.7D configuration

The simulation and previous works [2] show a high variation of pressure around 45 deg from the axis of the cylinders; therefore the analytical and the experimental analysis are focused at that point.
In order to have also a reference value of pressure, the data collected on the upstream cylinder are taken at the stagnation point, at 0 deg:

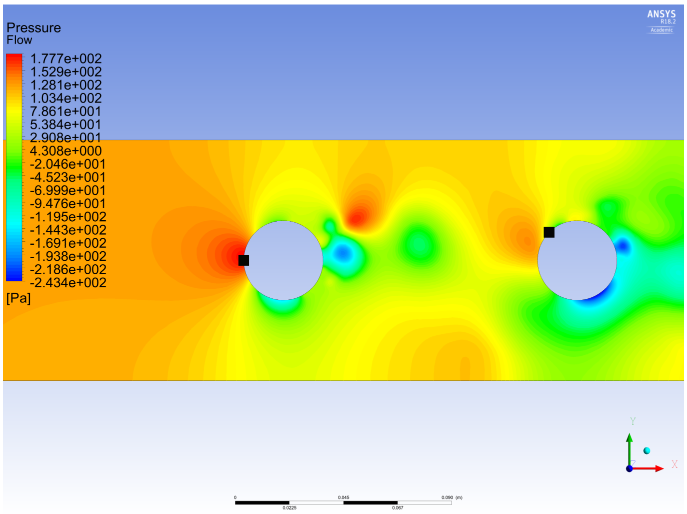

Figure 4.15: Points where the analysis is focused

4.3.5 Choice of the Instrumentation

From the Ansys simulation a qualitative expected pressure can be computed. Running the simulation up to a inlet velocity of $10\frac{m}{s}$ the maximum pressure fluctuation around the cylinder can be estimated in order to choose the pressure sensors. The point where the pressure is expected be higher around the cylinders is at the stagnation point on the upstream cylinder, while the fluctuations are stronger is at 45 deg from the axis [2]. Hence the pressure is taken at this point and Ansys gives the following result for a Re=46'456.

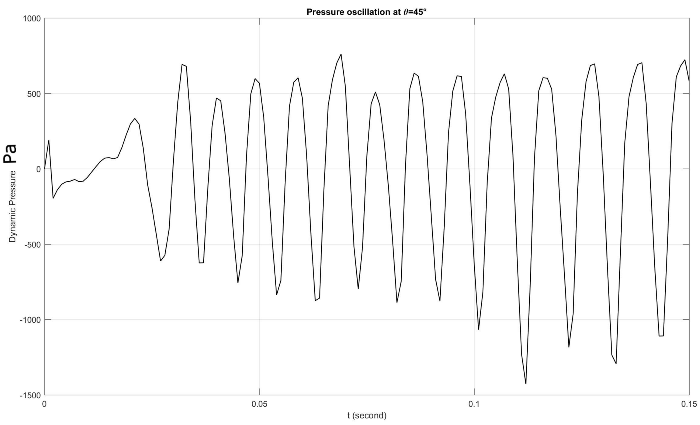

Figure 4.16: Pressure Oscillations at $\theta = 45\,\mathrm{deg}$

As it can be seen the maximum Dynamic Pressure on the cylinder is around 1000Pa 4.16, from this value the choice of the pressure transducer ha been guided.
From the furnisher *AllSensors* the pressure and the output play an important role into the choice of the transducer, the output indeed as to be in Voltage, and the resolution is obviously requested to be high.

Figure 4.17: selection of the specs of the pressure sensor, the dimension, the pressure range and the output have an important role into the choice of the transducer

The final choice went on the **Miniature Amplified Low Pressure Sensor**, in particular the **10 INCH-Dx-P4V-MINI** where its specs are resumed below:

Performance Characteristics for: 10 INCH-Dx-P4V-MINI

Parameter, NOTE 1	Minimum	Nominal	Maximum	Units
Operating Range, differential pressure		±10.0		mbar
Output Span, NOTE 5	±1.90	±2.0	±2.10	volt
Offset Voltage @ zero differential pressure	2.15	2.25	2.35	volt
Offset Temperature Shift (-25°C-85°C), NOTE 2			±20	mvolt
Offset Warm-up Shift, NOTE 3		±5		mvolt
Offset Position Sensitivity (±1g)		±5		mvolt
Offset Long Term Drift (one year)		±5		mvolt
Linearity, hysteresis error, NOTE 4		0.05	0.25	%fs
Span Shift (-25°C-85°C), NOTE 2			±1	%span

Figure 4.18: Specs of the pressure transducer used to measure the pressure fluctuation on the surface of the cylinders

The pressure transducers are hence placed inside the cylinder thanks to the sliders and connected to the wires using hand-made pins in the e-lab of the NRC and to the plastic tube that gives the reference pressure.

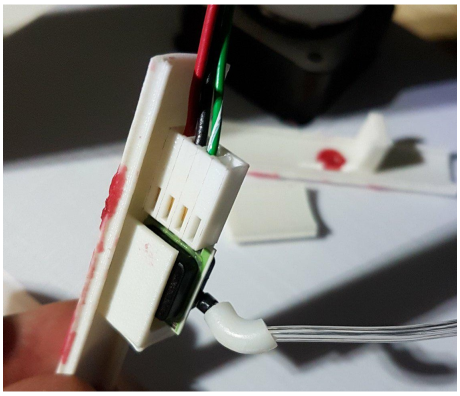

Figure 4.19: pressure transducer placed into the slider connected to the wires and to the plastic tube which gives the reference pressure

It can be seen in the figure a plastic elbow next to the tap for the tube. One problem faced during the assemblage was that the tube tended to bend too much next to the sensor, hence the elbow helps the tubes to follow a curvature and to avoid undesired bending that could spoil the income pressure.
Those elbows were printed also by a 3D printer in ABS. The plastic tubes were connected

thanks to a manifold hanged on the roof of the room that ensures the same pressure to 3 pressure sensors: one on the nozzle, one in the upstream cylinder and one in the downstream one.
The pressure given was first controlled by a pressure calibrator, after by the atmospheric pressure.
Indeed the experiment changed, while at the beginning I was focus to evaluate the pressure coefficient in order to check the correct configuration of the model, after the Sound Level Pressure was used to be check with the results in [2].
This change was due to the think that another pressure had to be check: the Dynamic Pressure, with the help of a Pitot Tube, making the experiment slower and too bulky.
Using the Sound Level Pressure, only the differential pressure is required, hence knowing the offset it can be scaled.
The pressure sensor presents 4 pins, but only the first three are used to get the data.

Thanks to the help of the staff at NRC a data acquisition wire has been built: the first and the second pin gives the current while still the second in combination with the third are connected to the data acquisition system.
During the first experiments another issue has been noticed: during the rotation of the cylinder the stiffness of the electric wire did not give enough freedom of movement, converting the torsional resistance into bending momentum on the pins, with the risk to break them.
To solve this problem I added free wires to plug to the previous one and to the transducer, reducing in this way the torsional resistance fig **??**. Those wires have been connected to

the Data Acquisition System and to the Power Supply.
The acquisition system has 4 channels, 2 of them are used for the pressure sensors.
In order to feed simultaneously the pressure sensors, a breadboard has been used in order to plug in parallel the transducers. The input Voltage is described in the specifics of the Pressure Transducers FIG, hence the given input power is $5V$.
A schematic connection is shown in the fig. 4.20

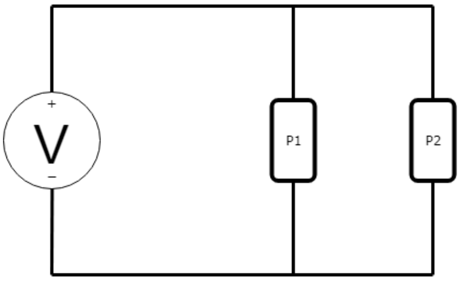

Figure 4.20: The simple schematic connection in parallel to connect the two pressure sensors to the power supplier.

The other pins (2 and 3) are connected to a Data Acquisition System (*Bruel and Kjaer 3050-A-040*), while the first channel is used to evaluate the input voltage, hence the offset to use once that the data are acquired. The connection is shown in fig. 4.21

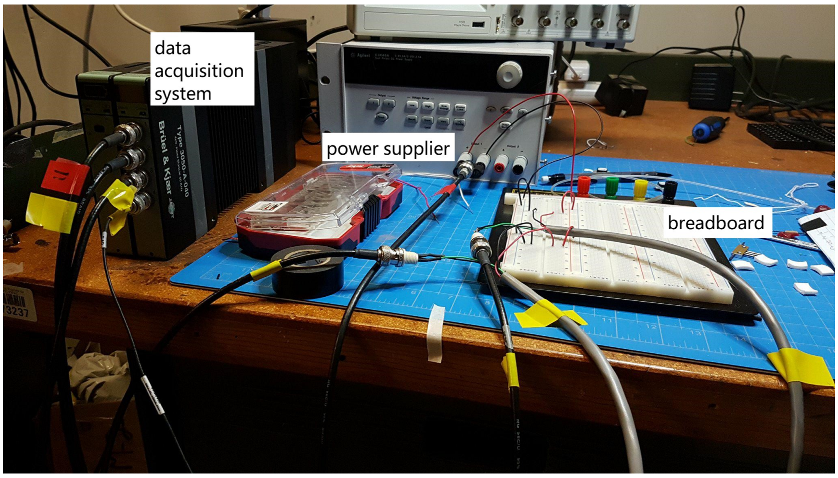

Figure 4.21: Connection to feed the transducers and to acquire the data into the Bruel&Kjaer

Since we are dealing with differential pressure sensors, I had to give a reference pressure. The sensor has 2 doors, hence it computes the difference of the pressure taken in each one.
Connecting the sensors using plastic tubes, through a manifold to a pressure calibrator

DPI 610 from **alpha company**,the reference pressure is checked.
Sometime the pressure calibrator was not available, hence the atmospheric pressure has been taken as the reference one.
For the latter case knowing the reference pressure was not important since the differential pressure oscillation was checked, and assuming that the atmospheric conditions were not changing in a short time (the experiment lasted not more that 1 minute).
The Nozzle, designed and printed by Dr. Syms, showed on its top a site where a third pressure sensor could be placed, in this way the pressure in the nozzle could be recorded and used as comparison in case one channel has to be sacrificed, since it is the only one that could not change its position in the set up.
The scheme of the hydraulic connection is simply showed in the fig. 4.22

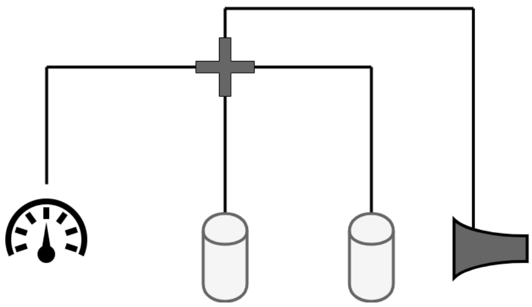

Figure 4.22: Schematic representation of the connection using plastic tubes and a manifold to give a reference pressure to the transducers.

Once that the pressure sensors were connected, in order to check their performance an application on an Ipad -**SonoScout**- made available by the NRC has been used.
This program can connect wireless with the acquisition system used and show in real time the output (set in voltage).
As expected from the specifics of the pressure sensors, when the differential pressure is

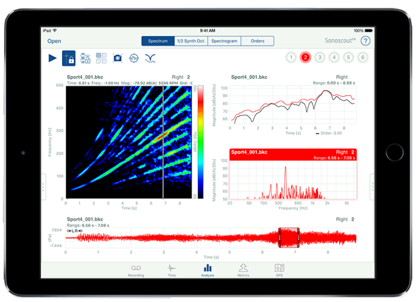

Figure 4.23: User Interface of **Sonoscout App** on Ipad, it gives the output in real time without and wire connection to the data acquisition system.

zero, hence the two doors of the transducer record the same pressure, the output voltage given was 2.25.
In this way I was able to establish the functionality of the circuit and of the entire instrumentation.
The speed of the flow could be set using a autotransformer.

Since the nozzle was not able to reach high velocities a compressor were attached by Dr.Syms, in this way the flow could reach speed of 30 $\frac{m}{s}$.
The autotransformer is not able to give the velocity of the field, hence a thermal anemometer has been mounted on the model in order to check the velocity of the flow.

Figure 4.24: The thermal anemometer and the pressure sensor placed on the nozzle to record the static pressure of the flow before the expansion.

On the table also a bendable structure were place in order to host a camera or a microphone.
The last one were used for my experiments, in particular a *DeltaTron Pressure-field, 1/4"* supplied by the National Research Center.
When all the material were checked working properly the set up was complete.
During the mounting parts different issues appears but thanks to the help of the staff of NRC/CNRC present in the labs I was able to tackle most of the problems I had during the set up.

The list of the material is presented below, while the pictures of them can be found in the appendix.

- Controllable Power Supply **VARIAC Autotransformer W5MT3**
- Cooling Fan **COFAN F-925H12B**
- Data Acquisition System **Bruel and Kjaer 3050-A-040**
- Driver **Arduino Uno**
- Limiter Switchers **RAM 1.4**
- Microphone 1/4" **Breul and Kjaer 4844A**
- Power Supply **AgilentE3648A**
- Pressure Calibrator **Omega DPI 610**
- Pressure Sensor **AllSensors DLH-L10D**
- I-Pad **SonoScout**
- Shield **CNC**
- Stepper motor **NEMA17**
- Thermal **PCE-423**

5 Evaluation

5.1 Results and interpretation

As explained before in order to know where but above the all, how to act to reduce the noise, the detection and the magnitude of the sound has to be done.
Once that the evaluation and the study is complete, the basic set up can be modified in order to understand how it can changes the measurements and the data.
My internship was mainly focused on the detection of the noise sources and on the analysis thanks to MatLab.

The experiment has been ran at the flow speed of $10\frac{m}{s}$.
The velocity of the flow is given by a controllable power supply *OHMITE* and checked by a thermal anemometer placed close to the upstream cylinder fig. 4.24.
The data are acquired by **SonoScout** in a wave form under *.wav* file and imported in MatLab were they have been studied.

The data got from the data acquisition system are in a wave form, and they describes the voltage oscillation.
The first channel as already described is the voltage input given to fed the pressure sensors, the second and the third the pressure oscillation on the cylinders, while the last one is the voltage oscillation recorded from the microphone.
Using the sensitivity of the devices given in the specs it is possible to convert the Voltage input into Pressure [Pa] then SPL [dB] using the equation 2.1:

$$Sensitivity = \frac{Units}{Output} \tag{5.1}$$

Table 5.1: Sensitivity of the Instrumentation used into the data analysis

Pressure Sensor	$0.887\frac{\mathrm{mV}}{\mathrm{Pa}}$
Microphone	$\frac{\text{Offset Voltage}}{\text{Operating Range}} = \frac{2.25}{10}\frac{\mathrm{Volt}}{\mathrm{mbar}}$

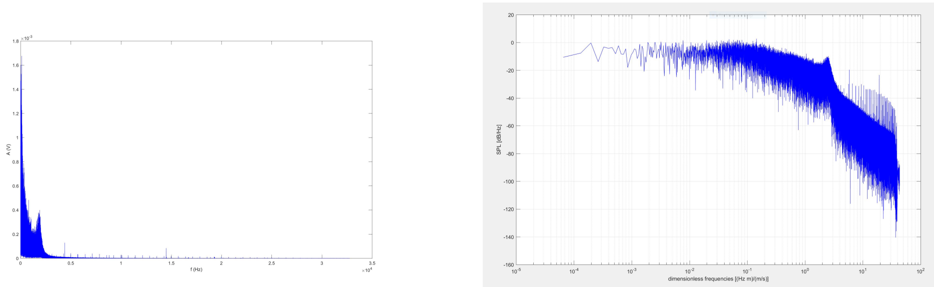

Figure 5.1: Pressure oscillation for the Upstream Cylinder at the stagnation point. On the left the FFT, on the right the Sound Pressure Level

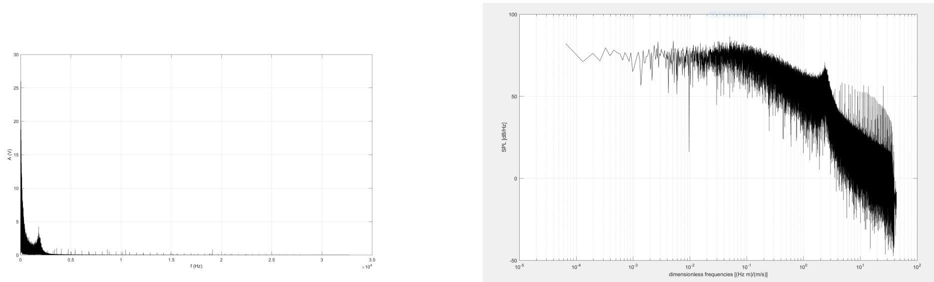

Figure 5.2: Pressure oscillation for the Downstream Cylinder at 45 from the axis. On the left the FFT, on the right the Sound Pressure Level

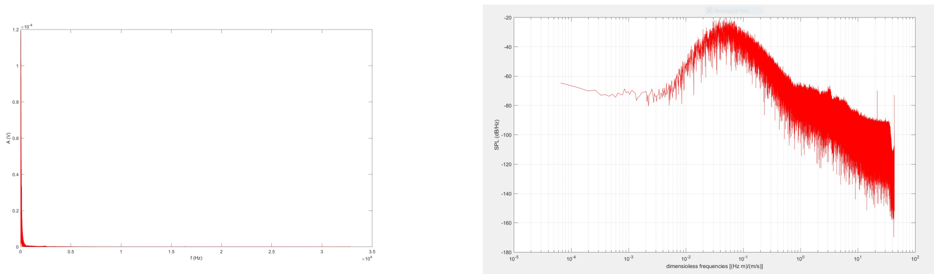

Figure 5.3: Pressure oscillation for the Microphone our from the flow placed at half of the distance between the cylinders. On the left the FFT, on the right the Sound Pressure Level

It can be seen how the microphone has, except for low frequencies due probably to the noise of the nozzle, a peak at a dimensionless frequency close to $10\frac{Hzm}{(m/s)}$.
Also the pressure fluctuations show a similar behavior at that frequency, that can induce to think a correlation, hence a correct set up.
The Fourier Transform Function (FFT) allows us to see the main frequencies responsible to the main noise, hence to act to reduce them.
The first channel is important to subtract to the data set of the pressure sensors the offset in order to avoid a highest frequency at zero.
Different noise can been seen especially at higher frequencies from the SPL graphs.
This problem can be solved extending the time of acquisition, and having more data that will reduce magnitude of the noise.
The microphone does not show any high frequency as the pressure sensors looking at the FFT, that can be causes by really low oscillation that the microphone cannot record, hence this frequency is not the main source of the noise.

Looking at the SPL it can be seen how, after a marked curve in the microphone SPL, the Pressure Level decreases with the frequency, except for a peak for a $3.196\frac{Hzm}{m/s}$.
This behavior is also present in the SPL of the downstream pressure sensor, where the peak appears at $2.38\frac{Hzm}{m/s}$.

Another experiment was ran increasing the velocity and not changing the set up. With the help of the compressor installed by Dr. Syms, the velocity recorder from the thermal anemometer reached the value of $23\frac{m}{s}$.
The data acquired and then scaled with my MatLab script are given in the fig.

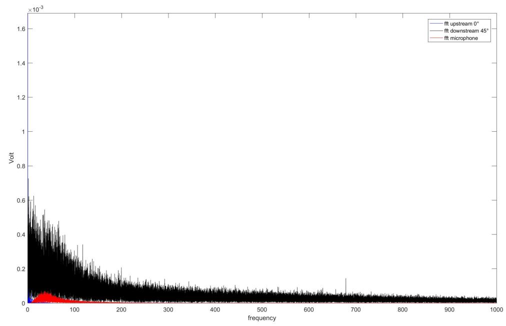

Figure 5.4: FFT for 23 $\frac{m}{s}$ of the 2^{nd}, 3^{rd} and 4^{th} channel, respectively upstream pressure, downstream pressure and microphone.

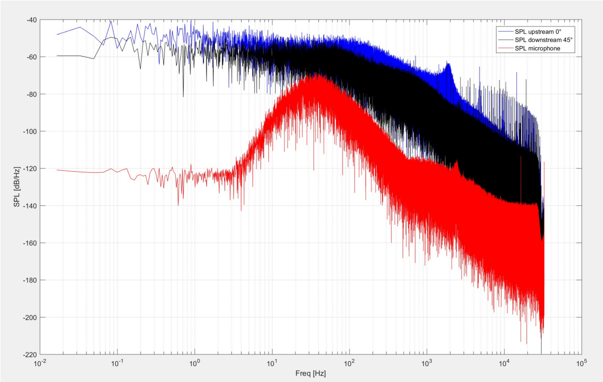

Figure 5.5: Sound Pressure Level of the 2^{nd}, 3^{rd} and 4^{th} channel, respectively upstream pressure, downstream pressure and microphone.

The shape for both situation show is the same, and in particular a correlation in peaks can be seen for the last set up (23 $\frac{m}{s}$) at around 20'000 Hz.
This can let think that the set up is satisfying, nevertheless a good choice of the instrumentation.

The not completely match of the frequencies can be due by a not precise position of the microphone.
Indeed the position of the microphone is object of studying in order to have a higher correlation and precision with the pressure sensors.
Turbulence phenomena can appear between the noise source and the microphone, changing the accuracy of the correlation between the two instruments.
The set up can be however used to test a speaker or a CNTs, keeping the same set up, in order to have an effective prove of the functionality of different configurations.

6 Conclusion

In conclusion it has been shown how the set up, in particular the geometry and the choice of the instrumentations have helped to reproduce previous works which have been already published and scientifically proven.
The set up has the advantage to change the configuration and to replace the instrumentation, just replacing the sliders and the sites for different devices as speakers or CNTs.

It is shown also how the fluctuation on a downstream cylinder is the main source of noise. Indeed the vortexes produced by the upstream cylinder, described by Von Karma REF, induce a pressure waves on the second cylinder.
That strong pressure variation in a short time can be seen with the Ansys simulation, and also recorder thanks to the pressure sensor flash mounted on the bluff body.
Thanks to this set up it is possible to measure the pressure fluctuation around the cylinder, increasing the precision with Arduino.

6.1 Future work

This set up can be used in the future in order to get more data at different configurations and different Reynold Numbers.
Furthermore the vortex shedding can be visualized with a camera and studied using the PIV technique as done by REF to predict the velocities and study in a better way the pressure fluctuations.

At the NRC/CNRC the set up in the soundproof wind tunnel can be in particular used to test CNTs for a reduced and more simple structure than a landing gear.
In this way the behavior of this material in a environment that simulates at best the landing phase of an airplane can be experienced and controlled easier than on a real size model, allowing to save time and money before acting on a real scale wind tunnel.

This project can lead an extreme useful development into aeroacoustic field, being able to detect the noise source and to act in order to reduce the acoustic emissions without interfering on the aerodynamics.

Bibliography

[1] R. H. Thomas, C. L. Burley, and C. L. Nickol, "Assessment of the noise reduction potential of advanced subsonic transport concepts for nasa's environmentally responsible aviation project," in *54th AIAA Aerospace Sciences Meeting*, 2016, p. 0863.

[2] A. Eltaweel, M. Wang, D. Kim, F. O. Thomas, and A. V. Kozlov, "Numerical investigation of tandem-cylinder noise reduction using plasma-based flow control," *Journal of Fluid Mechanics*, vol. 756, pp. 422–451, 2014.

[3] G. Xu and Y. Zhou, "Strouhal numbers in the wake of two inline cylinders," *Experiments in Fluids*, vol. 37, no. 2, pp. 248–256, Aug. 2004, ISSN: 1432-1114. DOI: 10.1007/s00348-004-0808-0. [Online]. Available: https://doi.org/10.1007/s00348-004-0808-0.

[4] L. Xiao, Z. Chen, C. Feng, L. Liu, Z.-Q. Bai, Y. Wang, L. Qian, Y. Zhang, Q. Li, K. Jiang, *et al.*, "Flexible, stretchable, transparent carbon nanotube thin film loudspeakers," *Nano letters*, vol. 8, no. 12, pp. 4539–4545, 2008.

[5] NRC/CNRC. (1999). Aerospace department, [Online]. Available: https://www.nrc-cnrc.gc.ca/eng/rd/aerospace/index.html (visited on 03/15/2018).

[6] D. R. D. Pijush K. Kundu Ira M. Cohen, *Fluid mechanics, fifth edition*.

[7] C. S. U. Donald E. Hall, *Basic acoustics*.

[8] A. Oberlin, M. Endo, and T. Koyama, "Filamentous growth of carbon through benzene decomposition," *Journal of Crystal Growth*, vol. 32, pp. 335–349, Mar. 1976. DOI: 10.1016/0022-0248(76)90115-9.

[9] C. Dekker *et al.*, "Carbon nanotubes as molecular quantum wires," *Physics today*, vol. 52, pp. 22–30, 1999.

[10] H. D. Arnold and I. B. Crandall., "The thermophone as a precision source of sound," *Phys. Rev.*, vol. 10, pp. 22–38, 1 Jul. 1917. DOI: 10.1103/PhysRev.10.22. [Online]. Available: https://link.aps.org/doi/10.1103/PhysRev.10.22.

[11] C. Doolan, "Flow and noise simulation of the nasa tandem cylinder experiment using openfoam," in *15th AIAA/CEAS Aeroacoustics Conference (30th AIAA Aeroacoustics Conference)*, 2009, p. 3157.

[12] M. Zdravkovich, "Review of flow interference between two circular cylinders in various arrangements," *Journal of Fluids Engineering*, vol. 99, no. 4, pp. 618–633, 1977.

[13] D. Lockard, M. Khorrami, M. Choudhari, F. Hutcheson, T. Brooks, and D. Stead, “Tandem cylinder noise predictions,” in *13th AIAA/CEAS Aeroacoustics Conference (28th AIAA Aeroacoustics Conference)*, 2007, p. 3450.

[14] Z. Yang, Z. Gu, J. Tu, G. Dong, and Y. Wang, “Numerical analysis and passive control of a car side window buffeting noise based on scale-adaptive simulation,” *Applied Acoustics*, vol. 79, pp. 23–34, 2014.